Advances in Concrete Construction, *Vol. 8, No. 4* (*2019*) *285-294*
DOI: https://doi.org/10.12989/acc.2019.8.4.285

A parametric shear constitutive law for reinforced concrete deep beams based on multiple linear regression model

Seyed Shaker Hashemi*[1], Kabir Sadeghi[2a], Saeid Javidi[1b] and Mahmoud Malakooti[1c]

[1]*Department of Civil Engineering, Persian Gulf University, Shahid Mahini Street, Bushehr, Iran*
[2]*Department of Civil Engineering, Near East University, ZIP Code: 99138, Lefkosa, TRNC, Mersin 10, Turkey*

(*Received September 19, 2018, Revised March 4, 2019, Accepted September 15, 2019*)

Abstract. In the present paper, the fiber theory has been employed to model the reinforced concrete (RC) deep beams (DBs) considering the reinforcing steel bar-concrete interaction. To simulate numerically the behavior of materials, the uniaxial materials' constitutive laws have been employed for reinforcements and concrete and the bond stress-slip between the reinforcing steel bars and surrounding concrete are taken into account. Because of the high sensitivity of DBs to shear deformations, the Timoshenko beam theory has been applied. The shear stress-strain (S-SS) relationship has been defined by the modified compression field theory (MCFT) model. By modeling about 300 RC panels and employing a produced numerical database, a study has been carried out to show the sensitivity of the MCFT model. This is performed based on the multiple linear regression (MLR) models. The results of this research also illustrate how different parameters such as characteristic compressive strength of concrete, yield strength of reinforcements and the percentages of reinforcements in different directions get involved in the shear behavior of RC panels without applying complex theories. Based on the results obtained from the analysis of the MCFT S-SS model, a relatively simplified numerical S-SS model has been proposed. Application of the proposed S-SS model in modeling and analyzing the considered samples indicates that there is a good agreement between the simulated and the experimental test results. The comparison between the proposed S-SS model and the MCFT model indicates that in addition to the advantage of better accuracy, the main advantage of the proposed method is simplicity in application.

Keywords: nonlinear analysis; RC deep beam; shear stress-strain; shear deformation; MCFT

1. Introduction

RC deep beams (DBs) "(RC-DBs)" are types of the structural members with specific complication and since they behave differently from the ordinary beams, special methods are required in the analysis and design of them.

Searching in the literature shows that some researches have been carried out experimentally or theoretically on the subject of shear in DBs. Amongst them, Malm and Holmgren (2008a, 2008b) performed laboratory tests to failure of ten large DBs cross-sections. Their measurements consisted of load-deformation curves, crack widths and crack patterns as well as the strain distribution near the supports. They observed that the truss model gave the best result for the beams with a higher reinforcement ratio that exhibited in a shear-compressive failure. All of the tests resulted in shear failure, either diagonal tensile failure or shear compressive failure, depending on the amount of reinforcement. Based on the analyses performed they also concluded that the plasticity-based model in Abaqus gives good agreement with the experiments related to crack pattern, load-displacement response, and estimated crack widths. Hu and Tan (2007) investigated the behavior and shear strength of large RC-DBs with web openings. They presented some test data for verifications of code predictions or strut-and-tie method (STM) results. Test results show that a web opening can reduce the ultimate strength of a large DB significantly if the web opening intersects the force path between the load point and the support. They observed that the crack patterns clearly illustrate an STM in large pierced DBs. Senthil *et al*. (2018) investigated numerically the deep beams with opening subjected to static monotonic loading. The simulations were carried out through the ABAQUS/CAE software and employing the Concrete Damaged Plasticity model as well as employing the Johnson-Cook material parameters. The obtained results were validated comparing with the experimental test results. They also studied the effect of span and shear span to depth ratio of the deep beams. Hars *et al*. (2007) have derived a mechanically-based efficiency factor for concrete in compression that is able to predict the actual behavior of structural cracked concrete. This approach predicts suitably the various potential failure modes and the development of the secondary shear cracks.

Code provisions for shear design of DBs have commonly developed from limited test results. There are also very few studies on the validity of shear-carrying

*Corresponding author, Assistant Professor
E-mail: sh.hashemi@pgu.ac.ir
[a]Professor
E-mail: kabir.sadeghi@neu.edu.tr
[b]M.Sc.
E-mail: javidi@mehr.pgu.ac.ir
[c]Assistant Professor
E-mail: malakooti@pgu.ac.ir

 ISSN: 2287-5301 (Print), 2287-531X (Online)

capacities of concrete and shear reinforcement in code provisions including STMs. Yang and Ashour (2008) investigated the effect of different parameters on the shear-carrying capacities of concrete and shear reinforcement in four building design code provisions (ACI 318-99, CIRIA Guide 2, ACI 318-05 and Eurocode2 (EC2)). They concluded that the code provisions generally fail to consider adequately the effect of different parameters on the shear strengths of concrete and reinforcement in DBs. Their investigation indicates that the shear capacities predicted from empirical code provisions and the STM of ACI 318-05 are more non-conservative in continuous DBs than in simple DBs, while the STM of EC2 is more non-conservative in simple DBs than in continuous DBs. In addition, a higher non-conservatism appears in STMs than in empirical formulae. Choubey *et al*. (2014) studied the influence of shear-span/depth ratio on the cohesive crack fracture parameters of concrete. They used the standard bending specimen geometry loaded with a four-point bending test. They found that the cohesive crack fracture parameters are independent of shear-span/depth ratio whereas, the initial cracking toughness of the material is dependent on the shear-span/depth ratio. In the case of simply supported DBs under concentrated loads with shear span to effective depth ratios (*a/d*) less than 2, the entire length of the shear span is considered as a disturbed region. To analyze and design this type of structural members, the STM proposed by ACI (2014), which initiated by Ritter (1899) can be used.

In RC-DBs, depending on the ratio of a/d and reinforcing steel mesh arrangement, the ultimate strength usually attained by shear controlling. The prediction of the ultimate strength and failure mechanism are complex because a different type of failure mechanisms has been observed for DBs in experimental tests (Ramadan and Abd-Elshafy 2017). Lu *et al*. (2010) developed a simplified technique by applying the softened STM to predict the shear strength and deflection of RC-DBs. Sanad and Saka (2001) applied artificial neural networks to predict the ultimate shear strength of a large number of RC-DBs.

Due to the distributed regions, the strain is distributed nonlinearly in the entire length of shear spans of RC-DBs and this type of beams do not obey the Euler-Bernoulli beam theory. The shear deformations play a significant role in the global behavior and ultimate strength of RC-DBs (Niranjan and Patil 2012). There are several behavior models to analyze the shear behavior of RC panels. Among them, Anderson *et al*. (2008) have submitted a model, which is developed to model the shear behavior of connections in RC structures. It is a relatively simple model and does not depend on several parameters. Belarbi and Hsu (1995) submitted another behavior model, which is known as the rotation angle softened-truss model (RA-STM). This model is more complex and considers the influences of some parameters of the RC panel.

Vecchio and Collins (1986) submitted an S-SS model based on the modified compression field theory (MCFT). This model is based on the equilibrium state of an RC member that is reinforced by an orthogonal reinforcing steel mesh. In this model, the ultimate tensile strength of concrete is taken into account. By employing the compatibility equations, Vecchio (2000) addressed the application of the MCFT, one of the first rotating crack models, in the analysis of DBs. The original constitutive relations were re-examined, and a crack width limit and residual tension term were introduced. To incorporate into a nonlinear finite element method (FEM), the model is capable to simulate sufficiently the strength, stiffness, ductility, and failure mode of lightly reinforced shear-critical test beams. Sectional analysis procedures based on the same model have been also made known to provide precise predictions of response. Ors *et al*. (2016) performed an analytical study on the modeling of shear critical RC beams by using the FEM. They submitted a mixed modeling approach in which the smeared cracking model was employed in conjunction with discrete cracking planes to model the concrete continuums in an effort to reach a better correlation with the experimental test data. The simulated results showed that their proposed modeling method is capable of better simulation of the observed experimental test response in terms of strength and stiffness, as well as the better simulation of the post-peak response of the beams.

Because of the high sensitivity of RC panels' global behavior to the shear deformations, applying an effective model to define the S-SS relationship is necessary. The accuracy of shear models depends on several parameters, besides the application of theories directly to create the S-SS model is time-consuming and is relatively complicated. In this research, the shear behavior of RC panels is studied focusing on the investigation of the main effective parameters in S-SS relations. A numerical S-SS model is proposed by means of analyzing the main parameters of RC panels. The proposed numerical model is based on the MCFT S-SS model and provides a numerical definition of MCFT.

2. Applied computer code

The computer code developed by Hashemi *et al*. (2016) is employed in this research. The mentioned code is programmed in MATLAB (2016) and the RC structural members are analyzed by employing the fiber theory and the Newton-Raphson nonlinear search method. By applying the fiber theory to the microscopic-based method, the computational expenses are reduced and the speed of the analysis is relatively increased. Besides the global and local behaviors of structural members can be analyzed by employing the mentioned computer code.

3. Bases of the proposed computer model

Based on the fiber theory, the DB is divided into some small segments. To remove the perfect-bond assumption, each reinforcement should be able to move independently of its surrounded concrete. In this way, therefore, the single degrees of freedom have been assigned to reinforcements. As illustrated in Fig. 1, the number of the degrees of freedom of RC structural members will be found by summing the degrees of freedom the concrete and

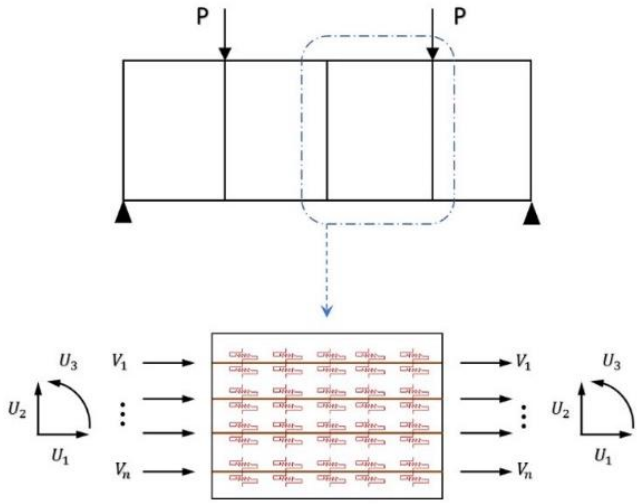

Fig. 1 Scheme of the applied RC-DB computer modeling

reinforcement. By applying a feeble form of equations, the continuous status of RC structural members will be converted to the discrete status. Gauss-Lobatto method is applied to determine the integration of the potential energy of discrete points. In the proposed numerical models in this paper, the potential energy of segments is determined at five discrete points. In the Gauss-Lobatto method, the integration of a polynomial equation of degree 2n-3 can be determined precisely where n represents the number of integration points (Pozrikidis 2005).

To consider the effects of shear and flexural deformations, Limkatanyu and Spacone (2002) and also Hashemi and Vaghefi (2015) submitted two formulations applying Timoshenko beam theory. To investigate the status of resistant and unbalanced forces, the Newton-Raphson nonlinear search method has been applied as an analytical basis. In this method, the stiffness can be reduced because of the correction of the stiffness matrix and this is the nonlinear behavioral origin of the analysis. Bond forces are considered as shear forces around the reinforcements and are determined by estimating the difference between reinforcement and concrete displacements. Bond forces are modeled by springs with nonlinear stiffness.

4. Modeling of materials

4.1 The constitutive law applied to concrete

The well-known uniaxial constitutive law of concrete proposed by Park and Kent (known as Park-Kent constitute law) is employed in this research to model the behavior of confined RC structural members considering the confinement effect of transverse reinforcements. Scott *et al*. (1982) edited this law and presented the behavior of concrete under tensile and compressive forces.

4.2 Constitutive law for reinforcement

The GMPF uniaxial constitutive law, proposed by Giuffrè and Pinto (1970), developed by Menegotto and

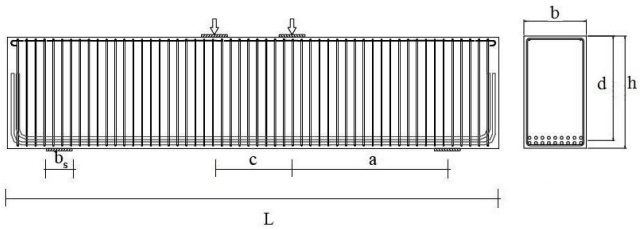

Fig. 2 Scheme of the dimensions and assembly of the tested samples (Salamy *et al*. 2005)

Pinto (1973), has been applied to model the behavior of reinforcements is employed in this research. In GMPF constitutive law, the unloading stiffness is assumed to be equal to the initial stiffness and the Bauschinger effect is considered. This model, which has been developed by Filippou *et al*. (1983), became more efficient by editing the isotropic strain hardening behavior in minor loadings.

4.3 Shear stress-strain (S-SS) model for concrete

To define the shear behavior of concrete in numerical models, MCFT S-SS model has been employed in this research. The initial model of MCFT was proposed by Vecchio and Collins (1986). This theory considers the effects of several parameters, which have high influences on the shear behavior of RC structural members. MCFT is based on the equilibrium equations of a concrete panel, which is reinforced by a reinforcing steel mesh. The RC panel behavior can be explained by the continuum-mechanics methodology. In this method, the RC panel is considered as a complex and its behavior is stated by the average response (Gil-Martin *et al*. 2011).

4.4 Bond stress-slip relationship

Eligehausen *et al*. (1982) proposed a bond stress-slip model. The tensile part of push curve can be used for the compressive part (Gan, 2000). When the confinement is not sufficient, in these circumstances, tensile and compressive parts are not the same. When the tension in the reinforcements exceed the yield limit, their lateral contraction is due to the tensile strain and their lateral expansions due to the compressive strain decrease and increase the bond tension between concrete and reinforcement respectively. It has been witnessed that these effects cannot affect more than 20% to 30% of the bond strength, even though these values are observed in large strains as well (Gan 2000).

5. Specifications of the experimental test

To verify the proposed model, the results of the experimental tests performed by Salamy *et al*. (2005) and Zhang and Tan (2007) were employed.

The examined samples (labeled as DB1 and DB2) are two RC-DBs tested by Salamy *et al*. (2005). These simply support beams are loaded with two increasing concentrated symmetric forces applied by a hydraulic jack up to the

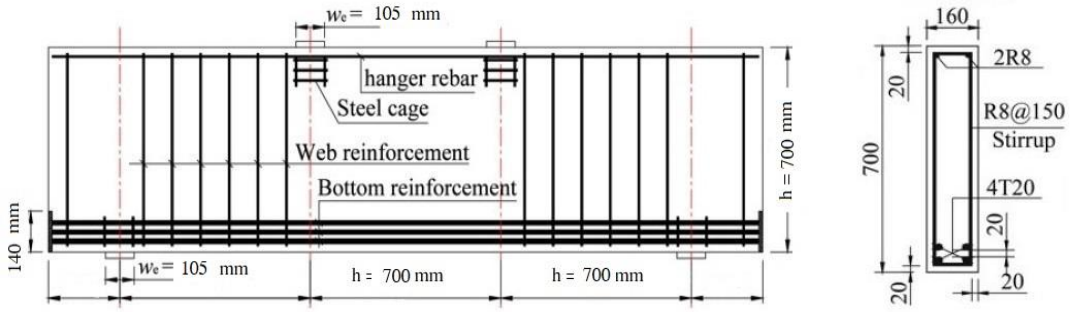

(a) 1DB70bw

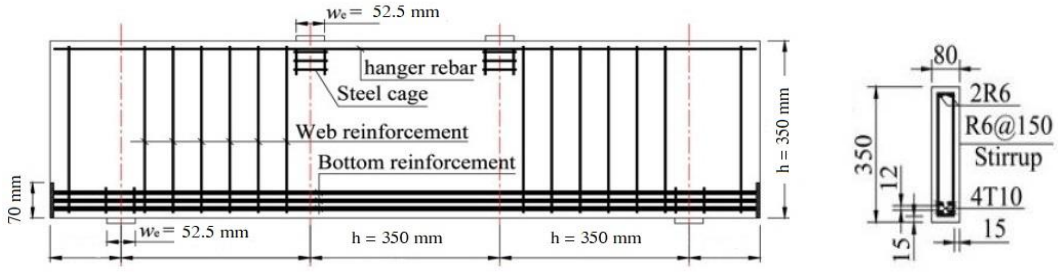

(b) 1DB35bw

Fig. 3 Reinforcement layout and cross-section of (a)1DB70bw and (b)1DB35bw (Zhang and Tan 2007)

Table 1 Dimensions of tested samples (in mm) (Salamy *et al*. 2005)

	a/b	*L*	*c*	*a*	*d*	*h*	*b*	b_s	f_c (MPa)
Sample 1	1.5	6650	1050	2100	1400	1505	840	350	23.5
Sample 2	1.5	3750	750	1500	1000	1105	600	250	28.7

Table 2 Reinforcement details of tested samples (Salamy *et al*. 2005)

	ρ_y (%)	ρ_x (%)	F_y (MPa)	Longitudinal reinforcements	Transverse reinforcements
Sample 1	0.4	2.05	397.5	18ϕ41, 2ϕ13	ϕ16@120
Sample 2	0.4	2.04	398	14ϕ32, 4ϕ13	ϕ13@100

failure, and the deflections are recorded at the middle of the span. The analysis of the crack pattern indicates that the failure mechanisms of both samples are of shear types. The scheme of the dimensions and assembly of the samples are demonstrated in Fig. 2.

Geometric characteristics of beams sections, materials specifications and the percentage of reinforcement in two perpendicular directions are submitted in Tables 1 and 2, respectively. Where in these Tables, f'_c represents the concretes' characteristic compressive strength, F_y represents the reinforcing steel's yield strength, ϕ represents the reinforcement's diameter (in mm), ρ_y represents the percentage of reinforcing steel bars in *y*-direction and ρ_x represents the percentage of reinforcing steel bars in the *x*-direction. The dimensions *L*, *c*, *a*, *d*, *h*, *b* and b_s depicted in Fig. 2 and Table 1 are defined as follows:

a: The distance between the point load and the support (center to center),

b: The width of the beam,

b_s: The width of the support,

c: The distance between the two point loads,

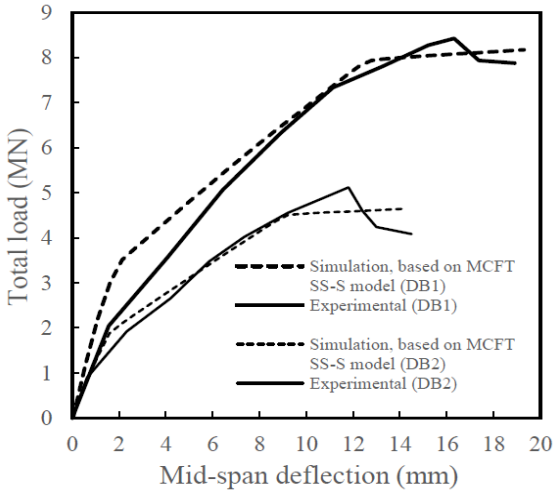

Fig. 4 Comparison of simulated results applying MCFT S-SS model with experimental test results

d: The efficient depth of the beam,

h: The depth (height) of the beam,

L: The span length of the beam.

For further assessment of the proposed model, the responses of two deep beams labeled "1DB70bw" and "1DB35bw", experimentally tested by Zhang and Tan (2007), were also deployed. Some details of these specimens are shown in Fig. 3 and more details about the geometry and materials and test results are given in the paper published by Zhang and Tan (2007).

6. Numerical simulation

The samples are numerically modeled according to the MCFT theory and applying the mentioned constitutive laws

Table 3 Comparison of simulated results using MCFT with the experimental test result

	Sample 1 (DB1)		Sample 2 (DB2)	
	Experimental test	Numerical simulation	Experimental test	Numerical simulation
E_1(GPa)	1.303	1.64	1.406	1.38
E_2(GPa)	0.51	0.427	0.418	0.345
Peak load (MN)	8.425	8.076	5.12	4.65

Table 4 The difference percentage between the simulated results using MCFT and experimental test results

	Sample 1 (DB1)	Sample 2 (DB2)
E1	21%	1.43%
E2	16.27%	17.46%
Peak load	4.14%	9.18%

in the computer code. Pushover analysis has been performed by controlling the displacement at the mid-span of the beam. In Fig. 4, the simulated results are compared with the results obtained from the experimental test of the samples DB1 and DB2.

Simulated results by applying the MCFT S-SS model have been compared with the experimental test result of DBs in Table 3. Where in this Table and also in Table 4, E1 represents the initial slope of the response curve and E2 represents the second slope of the response curve.

The difference between the simulated and experimental test results for E1, E2 and the peak load for both samples are submitted in Table 4.

The comparison between the simulated and experimental test results obtained for these two samples indicates that the shear behavior of this type of samples can be precisely determined by employing the S-SS models.

7. Application of the MCFT S-SS model in the analysis

Because of the high sensitivity of RC-DBs to the shear deformations, it is essential to apply an effective S-SS model with high precision in numerical modeling. The MCFT S-SS model reflects the influences of various parameters of RC panels in the determination of the shear behavior. In spite of its precision, the MCFT is relatively complicated; therefore, the creation of the S-SS model is time-consuming and complicated. To overcome this problem, Bentz and Collins (2001) developed the Membrane2000 software, which is able to make the S-SS model applying MCFT and some other theories.

In this research, the sensitivity of the MCFT S-SS model to the effective parameters has been investigated by modeling and analyzing some RC panels exist in Membrane2000 software. This model is classified as a simplified model due to the usage of a trilinear S-SS relation and the features of the introduced breaking points. Table 5 submits a summary of the database for the dependent and independent variables used in the analysis of the panels. In this Table, σ represents the standard deviation and N represents the number of data.

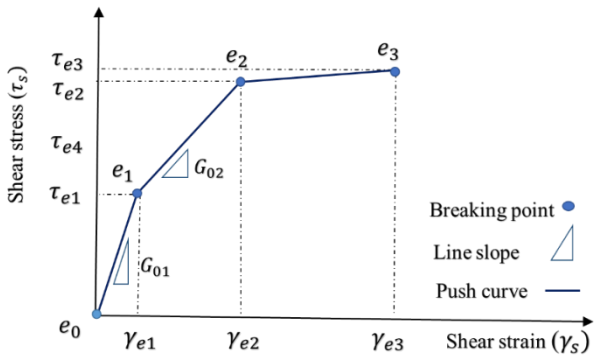

Fig. 5 Proposed S-SS model

8. Specification of the proposed S-SS model

MLR with the interaction of parameters has been deployed to analyze the data and predict the S-SS model with the characteristics illustrated in Fig. 5. In this

Table 5 Summary of database variables

	f'_c (MPa)				N	F_y (MPa)			
	Min	Mean	Max	σ		Min	Mean	Max	σ
τ_{e1}	20	29.79058	40	7.011878	(N=191)	300	324.0838	350	25.04886
τ_{e2}	20	30.49270	40	6.942592	(N=275)	300	347.6277	400	40.41715
τ_{e3}	20	30.44402	40	6.911382	(N=259)	300	348.8417	400	40.57019
G_{02}	20	30.11194	40	6.976859	(N=268)	300	350.9328	400	40.92868
γ_{e3}	20	30.49270	40	6.942592	(N=284)	300	347.6277	400	40.41715
	ρ_x (%)				N	ρ_y (%)			
	Min	Mean	Max	σ		Min	Mean	Max	σ
τ_{e1}	1	2.219895	3	0.661992	(N=191)	0.5	1.327225	3	0.71561
τ_{e2}	1	2.215328	3	0.658268	(N=275)	0.5	1.286496	3	0.674659
τ_{e3}	1	2.260618	3	0.623065	(N=259)	0.5	1.333977	3	0.668682
G_{02}	1	2.177239	3	0.655804	(N=268)	0.5	1.259328	3	0.630756
γ_{e3}	1	2.215328	3	0.658268	(N=284)	0.5	1.286496	3	0.674659

technique, the rate of contribution is determined for each parameter of the S-SS model and it makes possible to predict each breaking point applying simple and linear mathematical equations.

In this technique, a Y function is defined which depends on the variables X_1,X_2,X_3 and X_4. MLR with interaction is used to study this problem. The general form of a MLR model is submitted in Eq. (1).

$$Y = B_0 + B_1X_1 + \cdots + B_4X_4 + B_{12}X_1X_2 + \cdots + B_{34}X_3X_4 + \varepsilon \quad (1)$$

Where Y represents the dependent or response variable and X_1 to X_4 represent the independent or predictor variables. ε represents the error of model and B_0 to B_4 represent the regression coefficients. The coefficients are determined by applying Minitab17 software (2010) and the estimated model is expressed as follows

$$\hat{Y} = b_0 + b_1X_1 + \cdots + b_4X_4 + b_{12}X_1X_2 + \cdots + b_{34}X_3X_4 \quad (2)$$

Note that if the effect of interaction is major (p-value <0.05) in the interaction model, the main effects should be certainly submitted in the model. To find the best model with the least number of parameters, the ineffective parameters are omitted in the sequence; therefore, another variable cannot be eliminated from the model.

The numerical S-SS model can be determined by predicting the shear stress and shear strain at the breaking points. The results of the data analysis as the equations for the proposed S-SS model are submitted in Eqs. (3) to (9)

$$\tau_{e1} = 0.03843\, f'_c + 0.002025\, F_y + 0.1744\, \rho_x + 0.0227\, \rho_y - 0.000072\, f'_c.F_y + 0.001372\, f'_c.\rho_x + 0.000717\, F_y.\rho_y - 0.05675\, \rho_x.\rho_y \quad (3)$$

$$\tau_{e2} = -0.02431\, f'_c + 0.003517\, F_y + 0.393\, \rho_x - 0.688\, \rho_y + 0.01465\, f'_c.\rho_x + 0.01150\, f'_c.\rho_y + 0.007856\, F_y.\rho_y \quad (4)$$

$$\tau_{e3} = 3.315 - 0.1305\, f'_c - 0.006\, F_y - 0.184\, \rho_x + 0.065\, \rho_y + 0.000283\, f'_c.F_y + 0.02074\, f'_c.\rho_x + 0.00178\, F_y.\rho_x + 0.006413\, F_y.\rho_y \quad (5)$$

$$\gamma_{e1} = \tau_{e1}/G_{01} \quad (6)$$

$$G_{02} = -0.00862\, f'_c + 0.000617\, F_y + 0.1337\, \rho_x + 0.4825\, \rho_y + 0.002907\, f'_c.\rho_x + 0.003242\, f'_c.\rho_y - 0.00029\, F_y.\rho_y - 0.0406\, \rho_x.\rho_y \quad (7)$$

$$\gamma_{e2} = [(\tau_{e2} - \tau_{e1})/G_{02}] + \gamma_{e1} \quad (8)$$

$$\gamma_{e3} = 22.92 + 1.7621\, f'_c - 0.02849\, F_y - 10.92\, \rho_x - 16.31\, \rho_y - 0.002007\, f'_c.F_y - 0.2082\, f'_c.\rho_x - 0.0888\, f'_c.\rho_y + 0.01585\, F_y.\rho_x + 0.0096\, F_y.\rho_y + 4.974\, \rho_x.\rho_y \quad (9)$$

Where:

τ_{e1}: first breaking point shear stress,

γ_{e1}: first breaking point shear strain,

τ_{e2}: second breaking point shear stress,

γ_{e2}: second breaking point shear strain,

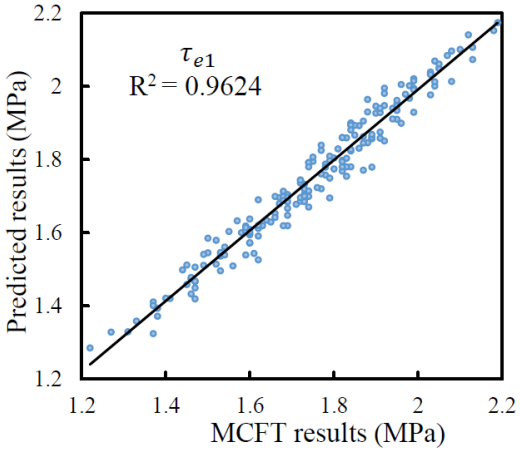

Fig. 6 τ_{e1}, the predicted results versus the results obtained by applying the MCFT

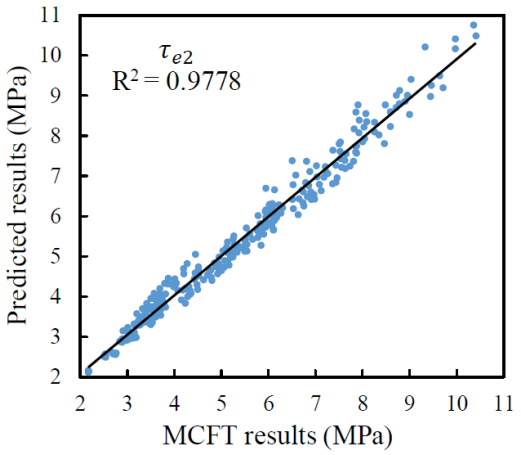

Fig. 7 τ_{e2}, the predicted results versus the results obtained by applying the MCFT

τ_{e3}: third breaking point shear stress,

γ_{e3}: third breaking point shear strain,

f'_c: concretes' characteristic compressive strength,

F_y: reinforcing steel bars' yield strength,

ρ_y: percentage of reinforcing steel bars in the y-direction,

ρ_x: percentage of reinforcing steel bars in the x-direction,

G_{01}: slope of the line of S-SS curve of concrete at first breaking point (shear modulus)

(see Fig. 5 and Eq. (10)),

G_{02}: slope of lthe ine of S-SS curve of concrete at second breaking point (see Fig. 5).

In the initial stages of loading and before the formation of the cracks, the reinforcing grid has no important influence on the shear behavior of RC panels. Thus, the initial slope of the S-SS model is determined using Eq. (10) based on the shear modulus of concrete.

$$G_{01} = E/2(1 + \upsilon) \quad (10)$$

With

$$E = \left(3300 \times \sqrt{f'_c} + 6900\right)(\gamma_c/23) \quad (11)$$

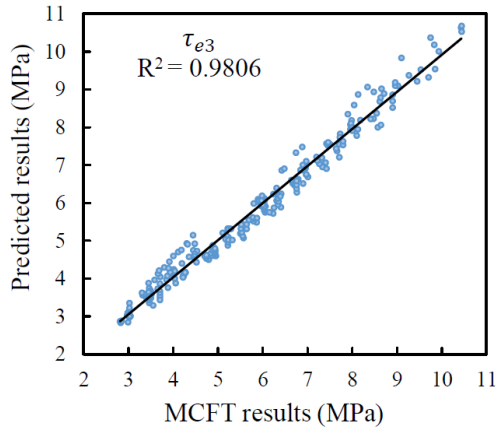

Fig. 8 τ_{e3}, the predicted results versus the results obtained by applying the MCFT

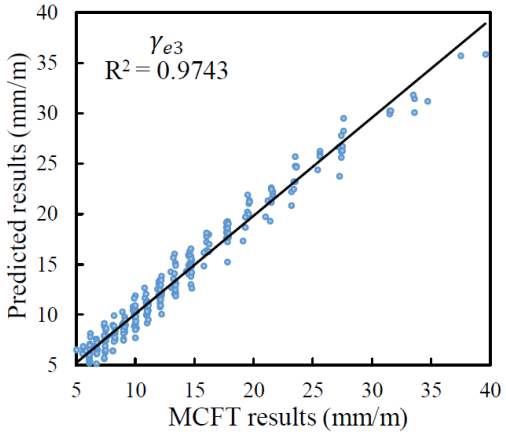

Fig. 9 γ_{e3}, the predicted results versus the results obtained by applying the MCFT

Where:
γ_c: concrete's specific weight,
υ: Poisson's ratio of concrete,
E: concrete's modulus of elasticity.

9. Comparison of the MCFT and proposed S-SS models

Each predicted parameter at the breaking points is compared to the values found by the application of the MCFT model as illustrated in Figs. 6 to 10. In all comparisons, the amounts of the coefficient of determination (R^2) indicate that the MCFT S-SS can be precisely predicted by applying the proposed numerical model.

10. Verification of the proposed S-SS model

In order to evaluate and validate the proposed S-SS model, the results of the experimental tests on RC panels under significant shear stress performed by Vecchio and Collins (1986) have been used. The specifications of the panels, as well as the details of laboratory test results, are

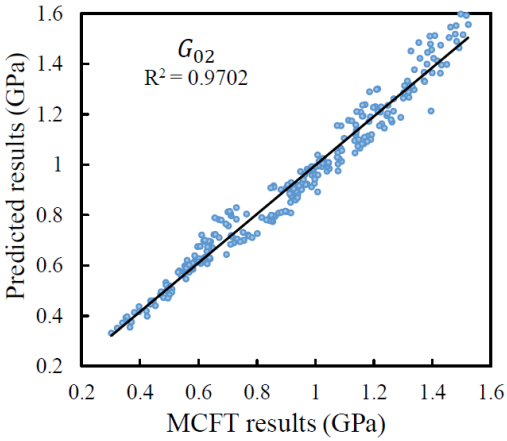

Fig. 10 G_{02}, the predicted results versus the results obtained by applying the MCFT

Table 6 Panels' specifications along with experimental and predicted values of τ_{e3} (Vecchio and Collins 1986)

Panel	ρ_x	F_{yz} MPa	ρ_y	F_{yy} MPa	f'_c MPa	τ_{e3} MPa (Experimental)	τ_{e3} MPa (Predicted)
PV2	0.0018	428	0.0018	428	23.5	1.16	1.22
PV4	0.0106	242	0.0106	242	26.6	2.89	2.77
PV6	0.0179	266	0.0179	266	29.8	4.55	4.86
PV10	0.0179	276	0.0100	276	14.5	3.97	3.82
PV11	0.0179	235	0.0131	235	15.6	3.56	3.96
PV16	0.0074	255	0.0074	255	21.7	2.14	2.31
PV19	0.0179	458	0.0071	299	19	3.95	3.92
PV20	0.0179	460	0.0089	297	19.6	4.26	4.42
PV21	0.0179	458	0.0130	299	19.5	5.03	5.44

given in Vecchio and Collins (1986) paper. The specifications of nine specimens along with the experimental ultimate shear stress and the results of the proposed S-SS model for τ_{e3} are presented in Table 6. The names of the panels match to the names mentioned in the paper of Vecchio and Collins (1986). In Fig. 11, the experimental test results are compared to the results of the proposed model for τ_{e3}. As it can be seen from this figure, there is a good agreement between the results obtained from the experimental test and the proposed model.

For further evaluation of the proposed S-SS model, by employing the specimen of PV20 of Vecchio and Collins (1986) laboratory tests, the result of the proposed S-SS model and the experimental results are compared, as illustrated in Fig. 12. The obtained results show a good agreement for various parameters including the first and second breaking point shear stresses (τ_{e1} and τ_{e2}) as well as for the shear stiffness.

The main application of the proposed S-SS model is for RC panels under significant shear forces. However, since the DBs with transverse reinforcements are very sensitive to the shear deformation, to express their realistic nonlinear behavior these RC members need S-SS model. Therefore, the proposed method is evaluated for DBs in this paper. In DBs, even with a relatively non-uniform distributed reinforcements, the proposed model is well able to predict their shear behavior.

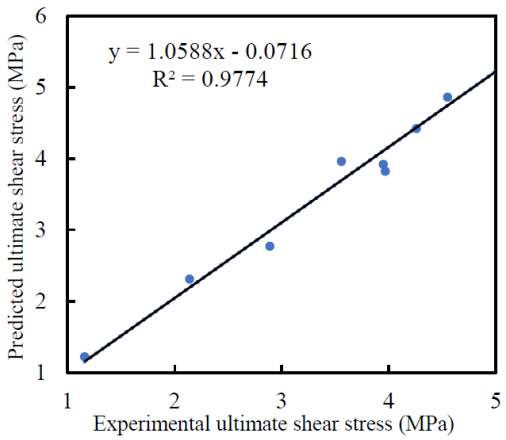

Fig. 11 Comparison of the experimental and predicted values of τ_{e3}

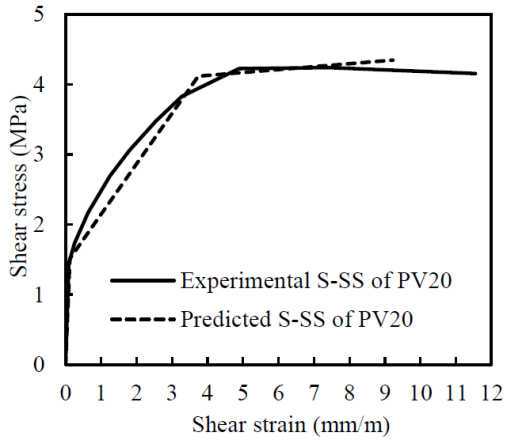

Fig. 12 Comparison of the experimental and the proposed S-SS curves

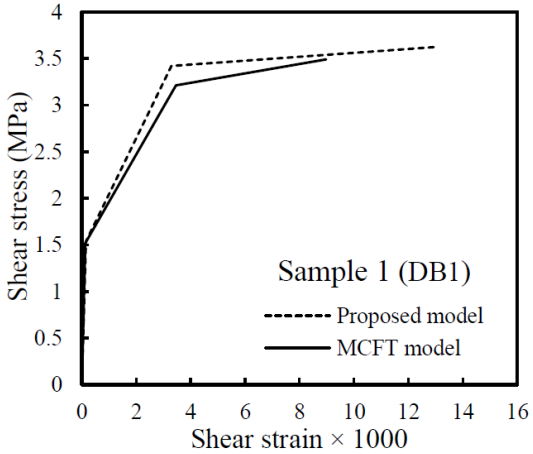

Fig. 13 Comparison of the MCFT and the proposed S-SS models for sample 1 (DB1)

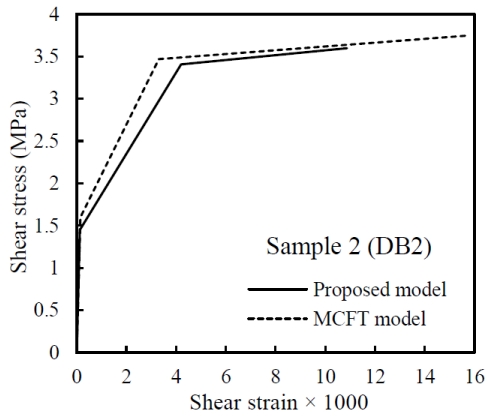

Fig. 14 Comparison of the MCFT and the proposed S-SS models for sample 2 (DB2)

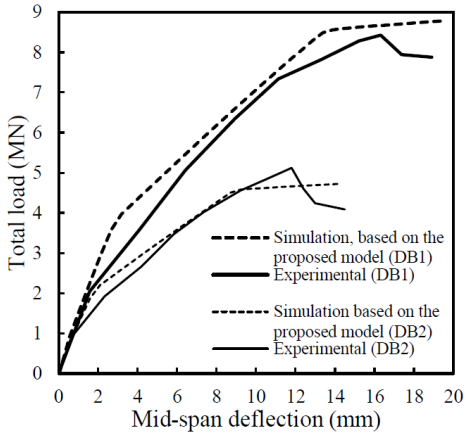

Fig. 15 Comparison of the numerical simulation results found by applying the proposed S-SS model with the experimental test result

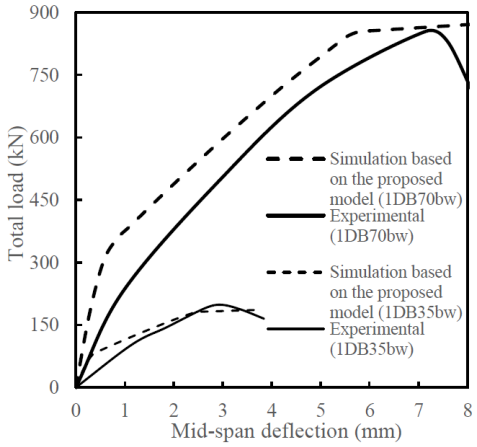

Fig. 16 Comparison of the numerical simulation results obtained by applying the proposed S-SS model with the experimental test result of 1DB70bw and 1DB35bw

The S-SS models for the samples DB1 and DB2 applying the proposed numerical model and the models made by applying the MCFT theory are compared and are submitted in Figs. 13 and 14.

By comparing the results of the proposed numerical S-SS model and MCFT model, it is concluded that push curve of the proposed model precisely matched with the MCFT model. To assess the efficacy of the proposed S-SS model, this model, as well as the MCFT model, have been employed in the numerical modeling of both samples separately. The simulated and experimental test results for the samples DB1 and DB2 have been compared as illustrated in Fig. 15.

Table 7 Comparison of simulated results using the proposed shear model with experimental test results

	Sample 1 (DB1)		Sample 2 (DB2)	
	Experimental test	Numerical simulation	Experimental test	Numerical simulation
$E1$(GPa)	1.303	1.34	1.406	1.36
$E2$(GPa)	0.51	0.445	0.418	0.349
Peak load (MN)	8.425	8.780	5.120	4.720

Application of the proposed S-SS model in modeling and analyzing the samples indicates that there is a good agreement between the simulated and the experimental test results. The simulated and experimental test results for both samples DB1 and DB2 are submitted in Table 7.

The percentages of the differences between the obtained results applying the proposed S-SS model and experimental test results for the initial slope (E1), the second slope (E2) and the peak load (ultimate strength) of both samples are submitted in Table 8.

The comparison between the values of the parameters submitted in Tables 4 and 8 indicate that the proposed S-SS model has a slightly better agreement with the results obtained from the experimental test compare to the MCFT model. Note that in addition to the advantage of better accuracy, the main advantage of the proposed method is simplicity in application.

The numerical and experimental response of the specimens "1DB70bw" and "1DB35bw" (Zhang and Tan 2007) are compared in Fig. 16. The good agreement between the simulated and the experimental test results shows that the proposed model, in addition to the high accuracy in predicting shear capacity, is able to employ the shear response to estimate the ultimate shear capacity of deep beams.

11. Conclusions

Since the application of the fiber makes possible to simulate numerically the RC structural members' behavior in the disturbed regions, it has been utilized in this research. The studies indicate that:

- By employing the MCFT theory, accurate results can be found with a relatively low computational expense.
- MCFT has submitted a good definition for RC panels and DBs' shear behavior, as reported in this research. This model is studied and the main influencing parameters on shear behavior and the influences of each parameter on the shear behavior of RC panels are submitted in the form of simplified mathematical equations.
- Based on the MCFT theory, the proposed S-SS model is defined by the simplest MLR models, which indicates the direct influence of each parameter on the shear behavior of RC panels and DBs.
- The proposed model submits a numerical definition of the MCFT S-SS model, without applying complicated and the time-consuming current MCFT relationships.

Table 8 The percentages of the differences between the obtained results applying the proposed S-SS model and experimental test results

	Sample 1 (DB1)	Sample 2 (DB2)
E1	2.7%	2.86%
E2	12.7%	16.5%
Peak load	4%	7.81%

- The numerical nature of the proposed model makes it suitable that easily be implemented in the numerical analysis software.

References

ACI (American Concrete Institute) (2014), Building Code Requirements for Structural Concrete and Commentary, ACI 318M-14, International Organization for Standardization, USA.

Anderson, M., Lehman, D. and Stanton, J. (2008), "A cyclic shear stress-strain model for joints without transverse reinforcement", *Eng. Struct.*, **30**(4), 941-954.

Belarbi, A. and Hsu, T.T. (1995), "Constitutive laws of softened concrete in biaxial tension compression", *Struct. J.*, **92**(5), 562-573.

Bentz, E. and Collins M.P. (2001), "Response-2000, Shell-2000, Triax-2000, Membrane-2000 user manual", University of Toronto, Toronto, Canada.

Choubey, R.K., Kumar, S. and Rao, M.C. (2014), "Effect of shear-span/depth ratio on cohesive crack and double-K fracture parameters of concrete", *Adv. Concrete Constr.*, **2**(3), 229-247.

Eligehausen, R., Popov, E.P. and Bertero, V.V. (1982), "Local bond stress-slip relationships of deformed bars under generalized excitations", *Proceedings of the seventh European Conference on Earthquake Engineering*, **4**, Techn. Chamber of Greece, Athens.

Filippou, F.C., Bertero, V.V. and Popov, E.P. (1983), "Effects of bond deterioration on hysteretic behavior of reinforced concrete joints", Earthquake Engineering Research Center, Report No. EERC 83-19, University of California, Berkeley.

Gan, Y. (2000), "Bond stress and slip modeling in nonlinear finite element analysis of reinforced concrete structures", MSc. Dissertation, Graduate Department of Civil Engineering University of Toronto, Canada.

Gil-Martin, L.M., Hernandez-Montes, E., Aschheim, M.A. and Pantazopoulou, S.J. (2011), "A simpler compression field theory for structural concrete", *Studi e Ricerche-Politecnico di Milano, Scuola di Specializzazione in Costruzioni in Cemento Armato*, 31, 11-41.

Giuffrè, A. and Pinto, P.E. (1970), "Il comportamento del cemento armatoper sollecitazioni cicliche di forte intensità", *Giornale del Genio Civile*, **5**(1), 391-408.

Hars, E., Niketić, E. and Ruiz, M.F. (2018), "Response of RC panels accounting for crack development and its interaction with rebars", *Mag. Concrete Res.*, **70**(8), 410-432.

Hashemi, S.S., and Vaghefi, M. (2015), "Investigation of bond slip effect on the PM interaction surface of RC columns under biaxial bending", *Scientia Iranica. Transaction A, Civil Engineering*, **22**(2), 388.

Hashemi, S.SH., Chargoad, H.Z. and Vaghefi, M. (2016), "A new approach for numerical analysis of the RC shear walls based on Timoshenko beam theory combined with bar-concrete interaction", *J. Rehab. Civil Eng.*, **4**(2), 79-92.

Hu, O.E. and Tan, K.H. (2007), "Large reinforced-concrete deep beams with web openings: test and strut-and-tie results", *Mag.*

Concrete Res., **59**(6), 423-434.
Limkatanyu, S. and Spacone, E. (2002), "Reinforced concrete frame element with bond interfaces. I: Displacement-based, force-based, and mixed formulations", *J. Struct. Eng.*, **128**(3), 346-355.
Lu, W.Y., Hwang, S.J. and Lin, I.J. (2010), "Deflection prediction for reinforced concrete deep beams", *Comput. Concrete*, **7**(1), 1-16.
Malm, R. and Holmgren, J. (2008a), "Cracking in deep beams owing to shear loading, Part 1: Experimental study and assessment", *Mag. Concrete Res.*, **60**(5), 371-379.
Malm, R. and Holmgren, J. (2008b), "Cracking in deep beams owing to shear loading, Part 2: Non-linear analysis", *Mag. Concrete Res.*, **60**(5), 381-388.
MathWorks, MATLAB (2016), The Language of Technical Computing, Version 8.3.0.532 (R2014a).
Menegotto, M. and Pinto, P.E. (1973), "Method of analysis for cyclically loaded RC plane frames including changes in geometry and non-elastic behavior of elements under combined normal force and bending", *Proc. IABSE Symposium on Resistance and Ultimate Deformability of Structures Acted on by Well-defined Repeated Loads*, International Association for Bridge and Structural Engineering. Zurich, Switzerland.
Minitab 17 Statistical Software (2010), Computer Software, State College, Minitab, Inc., PA, U.S.A.
Niranjan, B.R. and Patil, S.S. (2012), "Analysis of RC deep beam by finite element method", *Int. J. Modern Eng. Res.*, **2**(6), 4664-4667.
Ors, D.M.F., Okail, H.O. and Zaher, A.H. (2016) "Modeling of shear deficient beams by the mixed smeared/discrete cracking approach", *Hous. Build. Nat. Res. Center J.*, **12**, 123-136.
Pozrikidis, C. (2005), *Introduction to Finite and Spectral Element Methods using MATLAB*, Chapman & Hall/CRC Publisher, USA.
Ramadan, A.I. and Abd-Elshafy A.G.A. (2017), "Statistical prediction equations for RC deep beam without stirrups", *International Congress and Exhibition Sustainable Civil Infrastructures: Innovative Infrastructure Geotechnology*, Springer, Cham.
Ritter, W. (1899), "Hennebiques construction method", *Schweizerische Bauzeitung*, **17**, 41-43.
Salamy, M.R., Kobayashi, H. and Unjoh, S. (2005), "Experimental and analytical study on RC deep beams", *Asian J. Civil Eng.*, **6**(5), 409-421.
Sanad, A. and Saka, M.P. (2001) "Prediction of ultimate shear strength of reinforced concrete deep beams using neural networks", *J. Struct. Eng.*, **127**(7), 818-828.
Scott, B.D., Park, R. and Priestley, M.J.N (1982), "Stress-strain behavior of concrete confined by overlapping hoops at low and high strain rates", *J. Proc.*, **79**(1), 13-27.
Senthil, K., Gupta, A. and Singh, S.P., (2018), "Computation of stress-deformation of deep beam with openings using finite element method", *Adv. Concrete Constr.*, **6**(3), 245-268.
Vecchio, F.J. (2000), "Analysis of shear-critical reinforced concrete beams", *ACI, Struct. J.*, **97**(1), 102-110.
Vecchio, F.J. and Collins, M.P. (1986), "The modified compression-field theory for reinforced concrete elements subjected to shear", *J. Proc.*, **83**(2), 219-231.
Yang, K.H. and Ashour, A.F. (2008), "Code modeling of reinforced-concrete deep beams", *Mag. Concrete Res.*, **60**(6), 441-454.
Zhang, N. and Tan, K.H. (2007), "Size effect in RC deep beams: Experimental investigation and STM verification", *Eng. Struct.*, **29**(12), 3241-3254.